Neuron, Vol. 21, 1409–1422, December, 1998, Copyright ©1998 by Cell Press

The Retinotopy of Visual Spatial Attention

Roger B. H. Tootell,* Nouchine Hadjikhani, E. Kevin Hall, Sean Marrett, Wim Vanduffel, J. Thomas Vaughan, and Anders M. Dale
Nuclear Magnetic Resonance Center
Massachusetts General Hospital
Charlestown, Massachusetts 02129

Summary

We used high-field (3T) functional magnetic resonance imaging (fMRI) to label cortical activity due to visual spatial attention, relative to flattened cortical maps of the retinotopy and visual areas from the same human subjects. In the main task, the visual stimulus remained constant, but covert visual spatial attention was varied in both location and load. In each of the extrastriate retinotopic areas, we found MR increases at the representations of the attended target. Similar but smaller increases were found in V1. Decreased MR levels were found in the same cortical locations when attention was directed at retinotopically different locations. In and surrounding area MT+, MR increases were lateralized but not otherwise retinotopic. At the representation of eccentricities central to that of the attended targets, prominent MR decreases occurred during spatial attention.

Introduction

It is well known that our sensitivity to specific visual field locations is modulated by attention (reviewed by Posner and Petersen, 1990; Colby, 1991; Posner and Dehaene, 1994; Desimone and Duncan, 1995; Mangun, 1995; Maunsell, 1995). Spatial attention has been distinguished from other types of visual attention, such as attention to objects or features. Because spatial attention is so dynamic yet localized, it has often been described in metaphors such as a "spotlight" (Eriksen and Hoffman, 1973; Posner et al., 1980; Treisman and Gormican, 1988), a "searchlight" (Crick, 1984), or a "window" (Connor et al., 1997) of attention. Others have regarded such "top-down" metaphors as misleading, instead viewing attention as an "emergent process" (Desimone and Duncan, 1995).

In daily life, attention is normally drawn to a specific location in the visual field, followed almost immediately by a saccade to foveate that location. In the laboratory, such transient spatial attention effects can be studied in a sustained manner by having subjects fixate a specified point but direct and maintain their attention on a point specified elsewhere. This so-called "covert attention" paradigm has revealed a great deal about visual spatial attention in experiments including psychophysics, neuroimaging, and cortical electrophysiology.

*To whom correspondence should be addressed (e-mail: tootell@nmr.mgh.harvard.edu).

Despite this progress, many questions about the cortical organization of spatial visual attention remain unresolved. It would be especially helpful to know exactly which visual areas are modulated by spatial attention and how strong that modulation is in each area. Spatial attention has been studied in just a few of the ~30 areas of macaque visual cortex. What about spatial attention in each of the remaining areas? The role of spatial attention is even less clear in human visual cortex, since few prior studies have compared patterns of attention-related activity to the location of human cortical areas.

In both humans and macaques, prior studies suggest a hierarchical model in which spatial attention is, ironically, least prominent in precisely the area (V1) that has the most precise retinotopy and smallest receptive fields. Instead, spatial attention is thought to modulate activity in higher-order areas (e.g., V4 or IT), where receptive fields are much larger and retinotopy is less precise.

This hierarchical model of spatial attention is supported by a great deal of evidence across a wide range of experimental approaches, including macaque single units (e.g., Moran and Desimone, 1985; Luck et al., 1997), human event-related potentials (ERPs) (e.g., Mangun et al., 1993; Heinze et al., 1994; Mangun, 1995; Clark and Hillyard, 1996; Woldorff et al., 1997), and human neuroimaging studies (e.g., Corbetta et al., 1993; Heinze et al., 1994; Woldorff et al., 1997; Culham et al., 1998). However, there are also notable counter-examples to the hierarchical evidence in the macaque single unit evidence (e.g., Motter, 1993; Roelfsema et al., 1998), the ERPs (Aine et al., 1995), and the human neuroimaging (e.g., Shulman et al., 1997; Watanabe et al., 1998; D. Somers, personal communication).

Even if spatial attention effects were present and equally prominent in all visual cortical areas, this still leaves unresolved the retinotopic specificity of the effects within each area. For instance, how large is the "spotlight" of attention across the cortical map in each visual area? Does it expand drastically in higher-tier cortical areas, like the sensory-defined receptive fields? Single unit studies imply that the size of the attention spotlight may be directly related to the size of the receptive fields in each area (e.g., Connor et al., 1997; Luck et al., 1997), but this hypothesis has not been tested systematically in most cortical visual areas.

Human neuroimaging studies reported that spatial attention produces preferential activation in the hemisphere contralateral to the attended target (Mangun et al., 1993, 1997; Heinze et al., 1994; Mangun, 1995; Clark and Hillyard, 1996; Vandenberghe et al., 1996; Woldorff et al., 1997). Such demonstrations of cortical laterality are necessary but not sufficient to demonstrate retinotopy. For instance, cortical regions without demonstrable retinotopy, such as human MT+, can nonetheless show lateralized activity (Tootell et al., 1995a, 1998a). Furthermore, some visual cortical neurons are influenced by ipsilateral as well as contralateral stimuli, to varying extents and in different retinotopic locations (e.g., Van Essen and Zeki, 1978; Clarke and Miklossy, 1990; Tootell et al., 1998a).

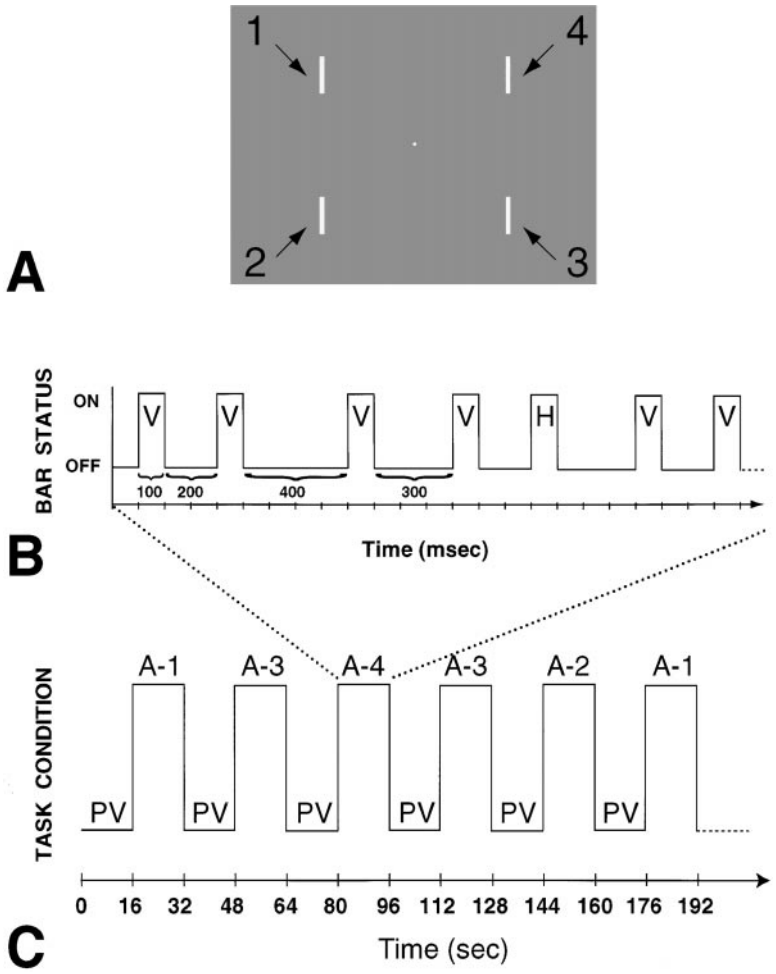

Figure 1. Diagram of the Stimulus and Timing in the Main Spatial Attention Experiment

(A) A picture of the stimulus at one point in time. A small central fixation point was always present, flanked by bars that were presented in a rapid repetitive sequence, in four locations (see below). The bars have been numbered here (see arrows) but were not in the actual stimulus.

(B) An example of the timing of the bar presentation in one quadrant, at a scale of milliseconds. For illustrative purposes, this time segment is sampled from the fourth quadrant during one of the "attend" trials ("A-4"; see below), but the timing and nature of the bar presentations were equivalent at all other times, in all quadrants.

(C) The overall timing of this experiment, on a time scale of seconds. Subjects either viewed the stimulus passively ("PV") or attended to one of the flashing bar targets ("A-1," "A-3′, etc.) in alternating blocks of trials.

Presumably, many of these questions could be resolved by using neuroimaging techniques in humans. Our approach here was to map spatial visual attention in direct comparison to the cortical retinotopy. To maximize relevance to the previous literature, we adopted a covert attention paradigm, using stimuli modeled after those used in previous ERP studies. To make the most revealing maps possible, we also used cortical flattening, improved retinotopic techniques, high-field (3T) imaging, and greatly expanded signal averaging.

Results

The main attention task is shown in Figure 1. It was designed to independently test the effects of (1) spatially selective attention, to each of four different locations, and (2) spatial attention, compared to passive viewing. During different 16 s epochs, the subject viewed a stimulus in which four bars (one in each quadrant) were repeatedly presented in a rapid "stream". Throughout the scan, the subject was required to maintain fixation on the central point and to either attend to the bars in a cued quadrant ("A-1," "A-2," "A-3," or "A-4," depending on the location of the cued quadrant), or to passively view the same display ("PV" condition). During any of the four "attend" conditions, the subject was required to indicate (via button press) when the bar appeared at a horizontal orientation. Performance data (percent correct) was reported to the subject after each scan. Importantly, the stimulus was identical during all these conditions. Full details of the attention task, and the retinotopic controls, are given in the Experimental Procedures.

Retinotopic Controls

Our analysis of the spatially selective attention results depended on localizing the retinotopic projection of the bar targets, from a purely sensory perspective. In the first of these control experiments, we presented the flashing bar targets during passive viewing conditions and compared the resultant activity to the activity produced while viewing the same stimulus without the bar targets (see Retinotopic Control Stimulus I in Experimental Procedures). An example from one subject is shown in Figures 2 and 3A. The peripheral flashing bars produced a pattern of activation, which was generally consistent with the geometry of the stimulus, relative to prior descriptions of the visual retinotopy. To test this relationship more precisely, we compared the activity maps produced by the bar targets (Figure 3A) to the overall maps of retinotopic eccentricity (Figure 3B) and

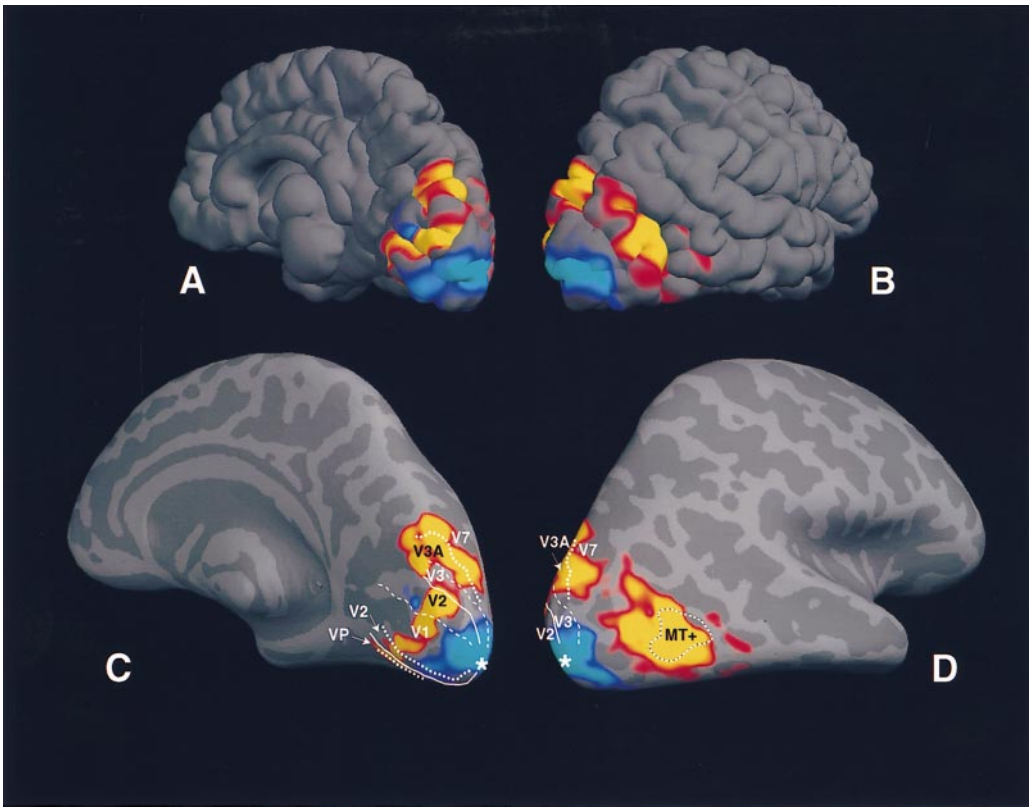

Figure 2. Retinotopy of the Bar Targets in Nonflattened Views of the Brain

This shows the results of a control experiment without attentional modulation, revealing the sensory projection of the bar targets relative to a uniform gray field (retinotopic control stimulus I). These fMRI maps are shown in a single right hemisphere, in both the normal folded state (A and B) and in the inflated state (C and D). The hemisphere is viewed from a medial–posterior viewpoint in (A) and (C) and from a lateral–posterior view in (B) and (D). In (C) and (D), sulci and gyri in the original folded brain are rendered in light and dark gray, respectively. MR signals that were significantly higher due to the flashing bars are coded in red-through-yellow pseudocolor. MR signals that were higher during the converse condition are coded in blue-through-cyan pseudocolor. In all retinotopic areas, the (yellow/red) activation produced by the bars was consistent with their retinotopic location at ~10.5°–11° eccentricity (see also Figure 3A). The (blue/cyan) "deactivation" was centered on the foveal representation (white asterisk). The borders of the major visual areas are labeled in (C) and (D).

polar angle (Figure 3C) in the same subject. As predicted, the activity map produced by the bar targets formed a chain-like pattern within the retinotopic areas. The long axis of this "chain" was centered on the isoeccentricity band at ~10.5°–11° (within green pseudocolor, Figure 3B), the eccentricity at which the bar targets were centered in the visual field (Figure 1A).

The polar angle retinotopy also makes a specific prediction about the projection of the bar targets. Instead of being uniformly thick and continuous as in the maps of isoeccentricity (Figure 3B), the thickness of this isoeccentricity "chain" should wax and wane as it crosses the adjacent retinotopic areas. It should be thinnest at the representations of the vertical and horizontal meridians, and thickest at the representation of intermediate (~45° oblique) polar angles—consistent with the location of the bar targets in the visual field. This variation in thickness should be most obvious in those areas with the most precise retinotopic map, especially V1 and, to a lesser extent, V2 (Tootell et al., 1997). This predicted activity pattern was seen in most cases (e.g., in V1 and V2 of Figure 3A).

In a prior study, we showed that a thin isoeccentric circle produced a much wider spread of activation in higher-order retinotopic areas such as V3A compared to that in lower-tier areas such as V1 (Figure 11 of Tootell et al., 1997). Such differences in the "cortical point image" support the generality (from macaque) that receptive fields in human V3A are larger than those in V1. Here, the discrete bar targets produced a similar effect. The "chain" of isoeccentric activation produced by the bar targets was relatively thin in areas V1, V2, and even V3/VP. However, it expanded greatly in areas V3A and V7 and to a lesser extent in V4v (see Figure 3A). This and similar data suggest that receptive field size is quite large in human areas V7 and V3A, medium sized in V4v, and smaller in V3/VP, V2, and V1.

The convergent information in Figures 3A–3C revealed the exact retinotopic projection of each of the bar targets used in our spatial attention experiment. Figure 3D shows this projection. Because activity in human MT+ is lateralized (Tootell et al., 1995a, 1997) but not obviously subdivided into upper versus lower visual field representations (Sereno et al., 1995; Tootell et al., 1995a, 1997; DeYoe et al., 1996), targets in both contralateral quadrants were predicted to project to MT+.

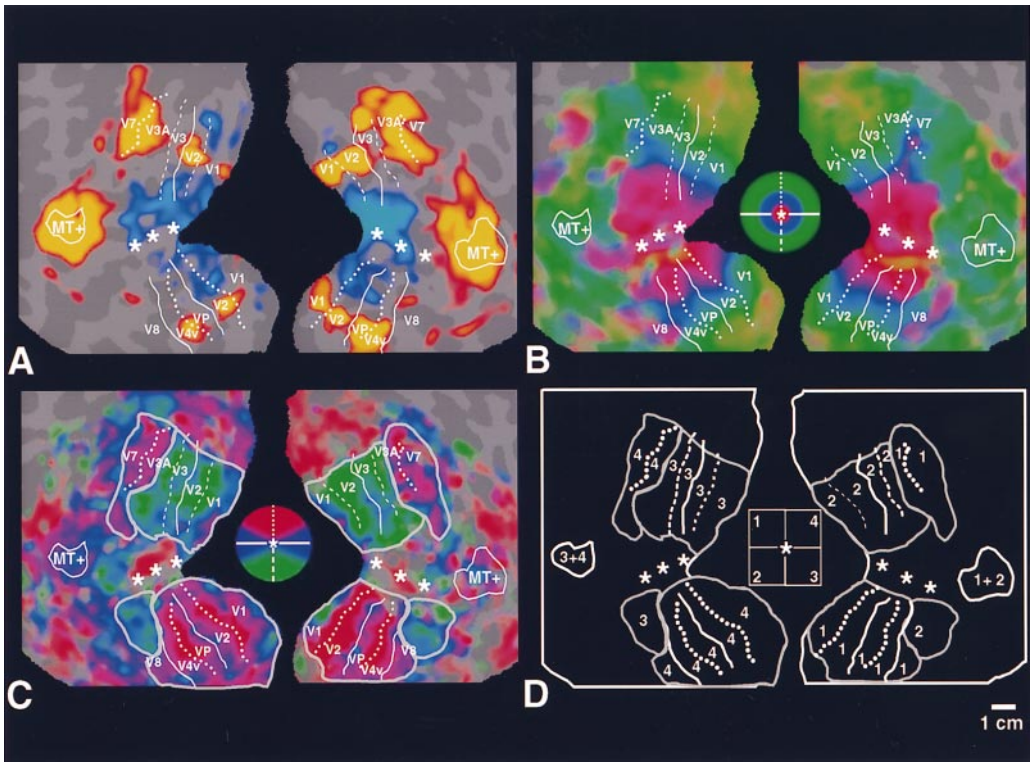

Figure 3. Retinotopic Localization of the Four-Bar Targets

Each panel shows flattened maps of the left and right hemispheres from a single subject, on the left and right side of the panel, respectively. (A) shows the same activity map as in Figure 2, plus data from the opposite (left) hemisphere. The phase-encoded maps of retinotopic eccentricity and polar angle (retinotopic control stimuli II) are shown in (B) and (C), respectively. In (D), the location of each of the bar targets in the visual field has been translated to their multiple representations in cortex. This retinotopic translation was based on the maps of phase-encoded retinotopy (B and C), retinotopic field sign (data not shown), and the map of activation due to the bars themselves (A). The bar targets are numbered according to the scheme in Figure 1A, redrawn in the central logo in (D). Gyri and sulci in the original (folded) brain are indicated as light and dark gray in the flattened cortical surface. The confluent foveal representation is indicated by a row of white asterisks across V1, V2, V3, etc. The borders of visual areas are shown by white lines (solid = horizontal meridian; dotted = upper visual meridian; dashed = lower vertical meridian; see logos in [B] and [C]). In (C) and (D), gray lines have also been drawn around each contiguous representation of the upper or lower visual fields, although this procedure artificially bisects V3A and V8. In (D), the numbers of the bar targets have also been placed at the projection of the bar targets. In other panels and in subsequent figures, the area names have instead been positioned at this same projection of the bar targets. The calibration bar indicates 1 cm, without correction for flattening distortion (average ~10%).

We also found a relative decrease in MR activity (blue through cyan) during the epochs containing the bar targets (see Figure 3A) in V1, V2, V3/VP, etc. However, this relative decrease did not occur in the retinotopic representations of the bar targets themselves. Instead, it occurred in the retinotopic representations of eccentricities closer to the fovea than the targets. This and similar foveal MR inhibitory effects are discussed in more detail below.

Spatially Selective Attention

Our main hypothesis was that attention to a specific visual field location produces higher MR activity in the retinotopically corresponding location of cortex, in at least some visual areas. Here, we tested that hypothesis, analyzing results from our main attention experiment (Figure 1). Figure 4 is an overview of the activity produced by attention to each of the four cued targets. Each comparison shows the significant differences in MR level during (1) attention to the target, indicated in the corresponding logo, minus (2) the average of all other conditions (i.e., attention to the targets in each of the remaining three quadrants, plus the passive viewing conditions). The subtraction condition here was deliberately open minded; in subsequent analyses, we compare the more specific activity produced only by attention to the different quadrants.

In general, the correspondence was quite good. Attention to a specific location in the visual field produced higher activity in the sensory representation of those same locations (see Figure 4). For instance, the retinotopic eccentricity of the attention-related activity was well centered on the "chain" of retinotopic eccentricity produced by the targets themselves. Also, the attention activity expanded dramatically in the higher-tier areas, such as V3A and V7, just as the sensory-based retinotopy did (cf. Figure 4C and Figure 3A). This suggests that the receptive field mechanisms underlying attention-based maps are closely related to those in the sensory maps.

However, the correspondence between the predicted and obtained attention retinotopy was not perfect. For

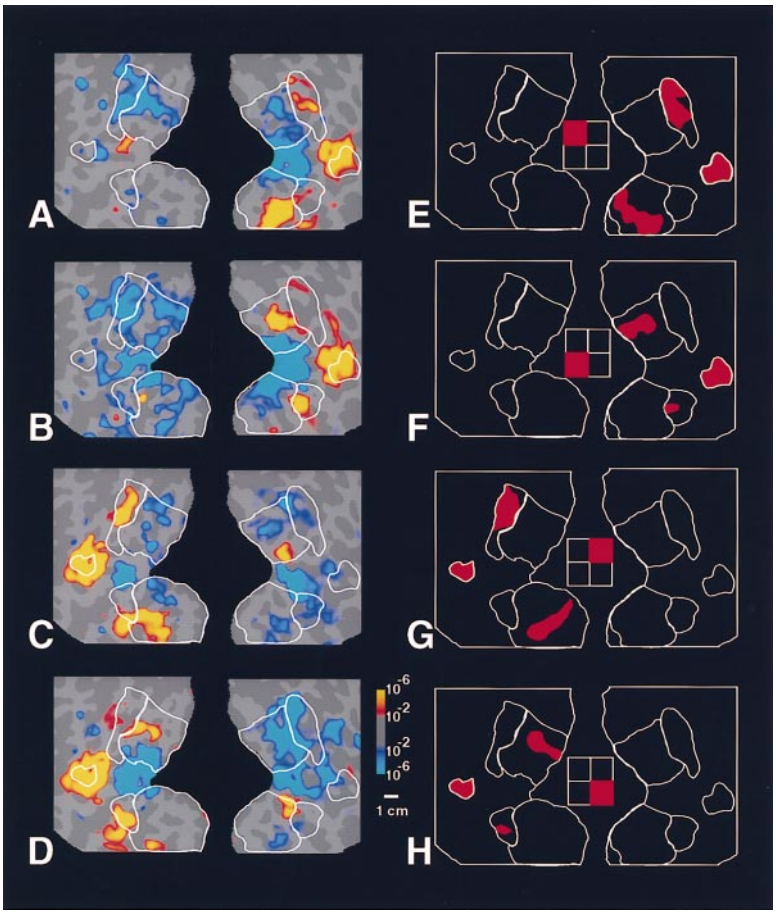

Figure 4. Overall View of the Retinotopy of Visual Spatial Attention

Each panel on the left (A–D) shows variations in MR activity produced by attention to a target in one quadrant, relative to all other conditions. All data are taken from the brain shown in Figure 3. The attended quadrant is indicated in the rectangular logo in the center of the right panels (attention directed to target in the upper left visual field [E]; lower left [F]; upper right [G]; lower right [H]). Based on the retinotopic analysis illustrated in Figure 3, the remaining parts of the diagrams on the right (E–H) show the topography of the sensory activity produced by each bar target (in red), relative to the diagram of the upper and lower visual fields in the polar angle map of the same subject (enclosed in white lines). Obtained MR activity that was significantly higher during attention to targets in the indicated quadrant is shown in red-through-yellow pseudocolor (see activity scale, bottom right) in the corresponding panels on the left. MR activity that was lower during attention to the indicated quadrant is rendered in blue-through-cyan pseudocolor.

instance, at this statistical threshold, the attention-related activity vanished toward the calcarine fissure, where V1 is normally located (see Figure 4 and below). On the other hand, the lateralized activity predicted (and found) in MT+ also extended well beyond that area, into the undefined cortical regions surrounding it. Finally, there were additional small patches of higher MR increases, which were not predicted by the retinotopy of the attended targets. In all panels of Figure 4, such "extra" patches were consistently located in retinotopic extrastriate cortex at a representation near 0.5° eccentricity, exactly opposite to the representation of the attended quadrant (i.e., in the hemisphere ipsilateral to the attended target and in the "wrong" superior–inferior quadrant). We do not yet understand these "extra" patches of increased MR signal.

Two types of evidence confirmed that the subjects maintained adequate fixation during this covert attention task. First, the retinotopic fMRI patterns themselves would have revealed any significant deviation from stable fixation. For instance, if the subjects had instead looked directly at the stimulus (rather than at the fixation point), the activity maps would have shown high activity in the representation of the fovea, rather than at 10.5°–11° eccentricity. No such artifacts were seen in attention maps.

Nevertheless, to address this issue more specifically, we measured eye movements in subjects while they performed the attention task, in the MR scanner. As shown in Figure 5, such tests confirmed that subjects maintained stable fixation on the central point while directing their attention to the peripheral targets, as in many prior covert attention studies.

Figure 6 shows the activity produced in our main attention paradigm in superior visual cortex. To reveal additional information, the format in Figure 6 differs from that in Figure 4 in several ways: (1) it is magnified, (2) the borders of visual areas are shown for comparison (rather than the contiguous representations of upper or lower visual fields), and (3) we used a more selective measure of spatial attention (attention to the cued quadrant, compared to activity in the nonattended quadrants, disregarding activity in the "PV" epochs).

As in Figure 4, selective attention to the upper versus lower visual field produced higher MR activity in the corresponding sensory representations of the upper and lower visual fields. Figure 6 shows further that this occurred even within a single area—in this case, V3A.

The attention-related retinotopy was approximately as orderly as the retinotopy itself. For instance, if one mentally adds the MR increases in the attention-related maps of the upper plus lower visual fields, one obtains an activity map almost indistinguishable from that produced by the (sensory-based) targets themselves, except in area V1. For example, if one adds the activity in Figures 6C and 6E, one gets approximately the map

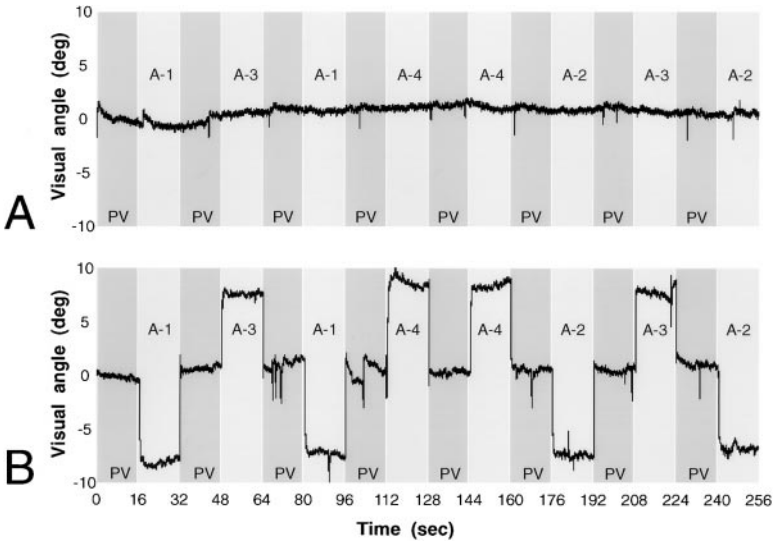

Figure 5. Subjects Can Perform the Covert Attention without Significant Eye Movements toward the Attended Targets

(A) Representative eye movements recorded while the subject was in the fMRI scanner, doing the main attention task (Figure 1). The trace is shown from the left eye, for the horizontal axis; traces for the other eye and axis were similar. Epochs of passive viewing (PV) are indicated as darker gray columns, and epochs of attention to a given quadrant (A-1, A-2, etc.) are shown as lighter gray columns. The quadrant-to-be-attended is numbered as in Figure 1A.

(B) Similar to (A), except that it was taken from a subsequent scan in which the subject deliberately looked at the attended target, as a control to calibrate the eye movements. The eye movements in (B) are quite obvious, relative to the stable fixation shown in (A).

In both (A) and (B), the minor deflections are due to eye blinks. The same randomization sequence was used here for both traces but not in the main experiments.

shown in Figure 6G, in extrastriate cortex. Similarly, the extrastriate activity in Figure 6D plus Figure 6F is nearly equivalent to that in Figure 6H. This attention-related activity was specific for both the eccentricity and the polar angle dimensions of the sensory retinotopy. The attention-related maps also respected the horizontal meridian in V3A (black line) quite well, as revealed by the maps of polar angle (Figures 6A and 6B). In some subjects, the attention-related activity spread into presumptively lower-tier areas such as V3 and V2 (e.g.,

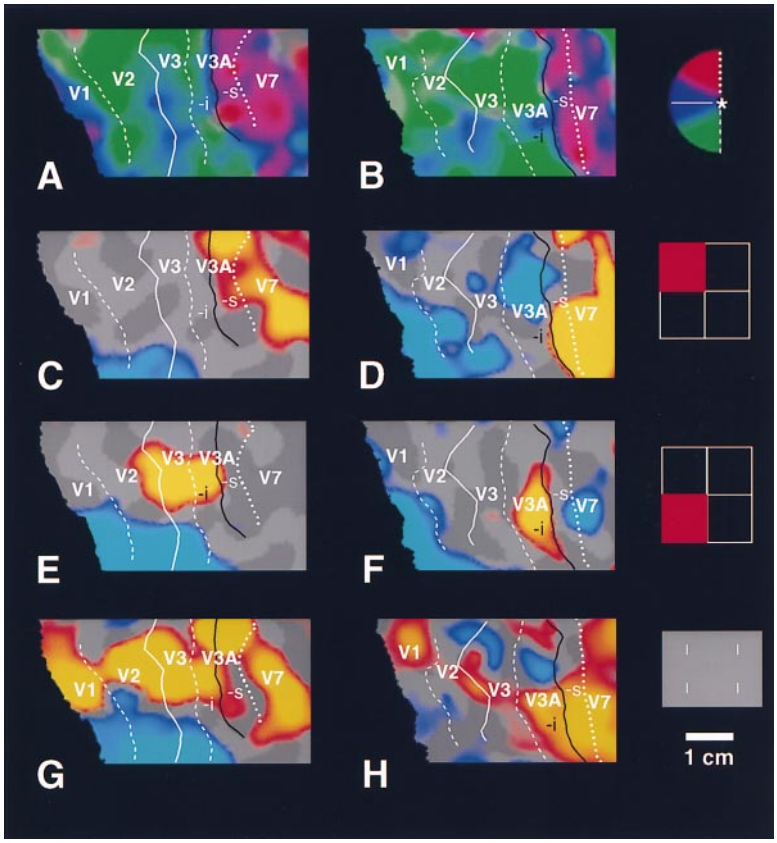

Figure 6. Selective Attention Retinotopy in Superior Occipital Cortex

(A), (C), (E), and (G) show a common region in the right hemisphere in one subject. (B), (D), (F), and (H) show a similar region from a second subject. The white lines are visual area boundaries corresponding to horizontal or vertical meridia, as in Figure 3. The solid black line is the representation of the horizontal meridian within area V3A. (A) and (B) show the polar angle retinotopy for each subject (see logo to the right of [B]). (C) and (D) show the activity produced during attention to a target in the upper left quadrant (see logo to the right of [D]), compared to the MR activity during attention to the three nonattended quadrants. (E) and (F) show the corresponding activity during attention to a target in the lower left quadrant. The pseudocolor activation scale for (C) through (F) is equal to that shown in Figure 4. (G) and (H) show the (sensory) retinotopic effects of the bar targets themselves, as in Figure 3A. In (C) through (F), the attention-driven MR increases (red-through-yellow) show a clear retinotopy. Attention to a target in the lower left quadrant produced higher activity in several lower field representations: the appropriate half of V3A in both subjects and V3 and V2 in one subject. Attention to the upper left quadrant produced higher activity in the upper field representation of V3A and in the adjoining upper field representation that comprises area V7. The retinotopic location of the attention-related effects (C–F) was quite consistent with the sensory retinotopy of the bar targets (G and H), except that little attention-related effect was found in lower-tier visual areas such as V1.

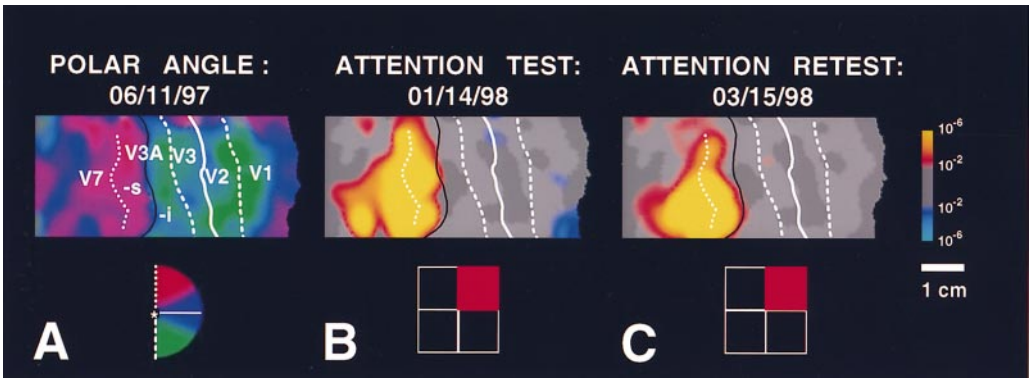

Figure 7. Test–Retest Reliability of the Spatial Attention Retinotopy

(A) through (C) show a single region of superior occipital cortex in the left hemisphere. (A) shows the map of retinotopic polar angle, and (B) and (C) show the activity produced by attention to a target in the upper right quadrant. The pseudocolor scale to the right is applicable to (B) and (C). The attention data was acquired during two different scan sessions, ~2 months apart (see dates above each panel). The polar angle map was acquired in a third session, ~6–8 months previously.

Figure 6E). However, unlike the sensory-based retinotopy (Figures 6G and 6H), the attention-related activity did not spread into V1 (Figures 6C–6F) at these statistical thresholds.

In the macaque, some groups have drawn a tentative visual area ("DP"), located immediately anterior to V3A, which includes a crude retinotopic representation of the upper visual field (Andersen et al., 1985a, 1985b; May and Andersen, 1986; Felleman and Van Essen, 1991). Other groups do not report this upper field area in macaque visual cortex (Gattass et al., 1988; Boussaoud et al., 1991).

In our more sensitive retinotopic maps from humans, we do see a crude representation of (at least) the upper visual field, located immediately anterior to, and apparently mirror-symmetric with, the upper field representation in V3A (Figures 6A, 6B, and 7A). This retinotopic representation has not been described previously in human visual cortex. Since the most similar macaque area ("DP") has not been defined consensually, and since DP was given the lowest possible confidence rating even by Felleman and Van Essen (1991), we have given the human area a different name ("V7") rather than presume homology to macaque DP.

Our most crucial comparisons (e.g., Figure 1) were always acquired within the same scan session. However, these experiments required comparisons between many hours of scanning data—enough data so that it could not be acquired within a single scan session. Nevertheless, Figure 7 shows that even comparisons of data across different scan sessions are not a cause for concern. Maps of selective attention in V3A and V7 (calculated as in Figure 6) were nearly identical, even when they were acquired in entirely independent experiments, done months apart. Furthermore, both of those attention maps were nicely aligned with the map of polar angle retinotopy, which was also generated months previously.

The results of corresponding tests in inferior occipital cortex (Figure 8) were conceptually equivalent to those shown above in superior occipital cortex (Figures 6 and 7). Again, attention to a target in the upper visual field produced higher MR activity in the contralateral representations of the upper visual field, at the predicted eccentricity (Figure 8B). Again, this activity was most robust in presumptively higher-tier retinotopic areas (e.g., VP, V4v, and V8), but it was less prominent in V2 and nearly insignificant in V1. Conversely, attention to a target in the lower visual field produced higher MR activity in the small contralateral representation of the lower visual field, located in area V8 (Figure 8C).

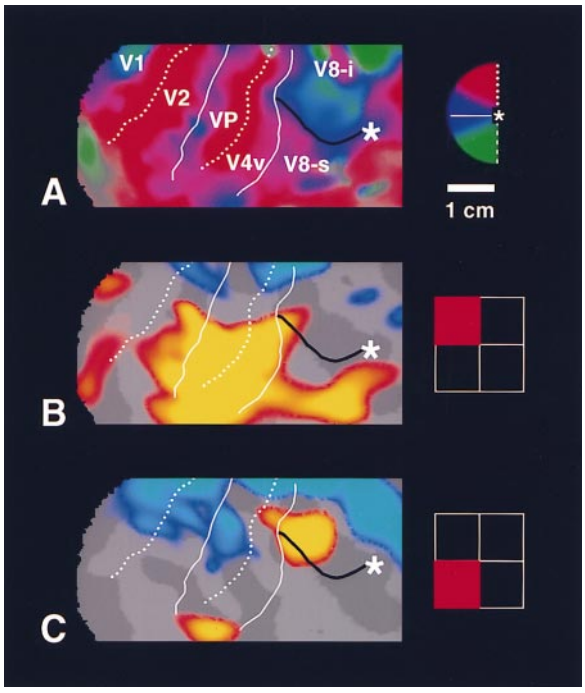

Figure 8. The Retinotopy of Spatial Attention in Inferior Occipital Cortex

The format and experiment are similar to those described in Figures 6 and 7. One region of cortex is shown in all three panels. (A) shows the polar angle retinotopy, (B) shows the map of attention to the upper visual field, and (C) shows attention to the lower visual field. The pseudocolor activity scale is equivalent to that in Figures 4 and 7.

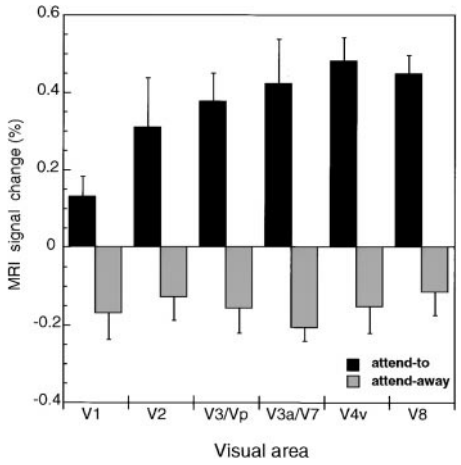

Figure 9. Averaged MR Signal Change during Spatially Selective Attention

The black bars represent the relative level of MR signal change during spatially selective attention in the retinotopically predicted region (the "attend-to" condition) within each visual area indicated on the x axis. The gray bars represent the MR responses in the same cortical regions when attention is directed toward the diametrically opposite quadrant (the "attend-away" condition). Zero on the y axis represents the mean MR level during passive viewing. The error bars represent one standard error. Data from V3 and VP are combined because in humans these are increasingly regarded as two parts of a single cortical area. Data from areas V3A and V7 were combined for technical rather than theoretical reasons.

To test these impressions further, we measured the MR responses during spatial attention in (1) retinotopically predicted regions of interest (ROIs) within each area (the "attend-to" condition) and in (2) equivalent ROIs during attention to the opposite ("attend-away") quadrant, as a control. Responses were calculated independently in each visual area. However, signals were combined from all four attend-to (and attend-away) quadrants, for the purposes of signal averaging.

Figure 9 shows such results across subjects ($n = 6$). As in the individual activity maps, spatial attention to a given location in the visual field produced MR increases in the retinotopic projection of that location. Consistent with the individual activity maps and most previous studies, V1 showed the least signal change (mean = 0.13%), and presumptively higher-tier areas (e.g., V8, V4v, V7, and V3A) showed larger changes (means = 0.38%–0.48%). To test the statistical significance of these effects, we performed a one-way ANOVA, with visual area as a within-subject factor. A significant mean signal increase was observed across areas in the attend-to condition relative to passive viewing [$F(1,5) = 29.418$, $p < 0.005$]. The analysis also showed a significant effect of visual area [$F(5,25) = 4.565$, $p < 0.005$]. Further analysis confirmed a greater attention effect in higher-tier areas relative to V1. More precisely, a pairwise comparison of activation in the attend-to condition between visual areas (paired t test assuming unequal variance) showed a significant difference between area V1 and areas V3/VP ($p < 0.05$), V3A/V7 ($p < 0.05$), V4v ($p < 0.001$), and V8 ($p < 0.001$). No other pairwise comparisons yielded significance beyond $p < 0.1$.

The extensive signal averaging in Figure 9 also revealed additional aspects of the data that were not so obvious in the individual activity maps. Not only did the MR signals increase during the attend-to conditions (relative to passive viewing), but they also decreased during the attend-away conditions. Unlike the MR increases, the decreases were relatively constant in amplitude across visual areas. These results were confirmed by a one-way ANOVA on the activations in the attend-away condition, with visual area as a within-subject factor. This analysis showed a significant mean signal decrease across areas in the attend-away condition relative to passive viewing [$F(1,5) = 16.511$, $p < 0.01$] but no significant effect of visual area [$F(5,25) = 0.447$, $p = 0.811$]. Reflecting the opposing signal increases and decreases, the difference between attend-to and attend-away conditions was significant in every area, based on a two-sample t test assuming unequal variances [6 subjects; V1: $t(10) = 3.48$, $p < 0.005$; V2: $t(10) = 3.08$, $p < 0.01$; V3/VP: $t(10) = 5.73$, $p < 0.001$; V3a/V7: $t(10) = 5.23$, $p < 0.001$; V4v: $t(10) = 6.99$, $p < 0.001$; and V8: $t(10) = 7.42$, $p < 0.001$].

Consistent with our retinotopic predictions (Figure 3), selective attention to targets in both inferior and superior contralateral quadrants produced overlapping activity in MT+ (see Figure 10). Although there were hints of a topographic variation that were dependent on target position within the contralateral visual field, these variations were not systematic across subjects. When attention was directed to the ipsilateral visual field, there were also MR signal decreases in MT+ in some subjects (e.g., Figures 10). This lateralization of attention-related activity also extended well into the cortical regions surrounding MT+.

To test the reliability of these results across subjects, we performed a two-way ANOVA, with the first factor being stimulus location (each of the four quadrants) and the second factor being visual area (right and left hemisphere MT+) as within-group factors (see Figure 11). This repeated measures ANOVA confirmed a significant interaction of stimulus location by visual area [$F(3,15) = 21.3$, $p < 0.001$].

Attention versus Passive Viewing

Instead of concentrating on the retinotopy of spatial attention, one might ask about the relative activity levels during spatial attention per se (that is, irrespective of target location), compared to passive viewing of the same stimuli. This was the experimental approach in earlier neuroimaging studies of visual spatial attention (e.g., Corbetta et al., 1993, 1995; Nobre et al., 1997; Culham et al., 1998). Our main attention experiment (Figure 1) was designed to address this question as well (see Figure 12A). Surprisingly, most of the significant activity in this comparison was relatively lower during spatial attention, compared to that occurring during passive viewing conditions. Though initially counterintuitive, this result is in fact perfectly compatible with the attention-related MR increases described above.

It is easiest to understand these results when they are considered separately in two cortical subdivisions: (1) regions that showed prominent MR increases in the

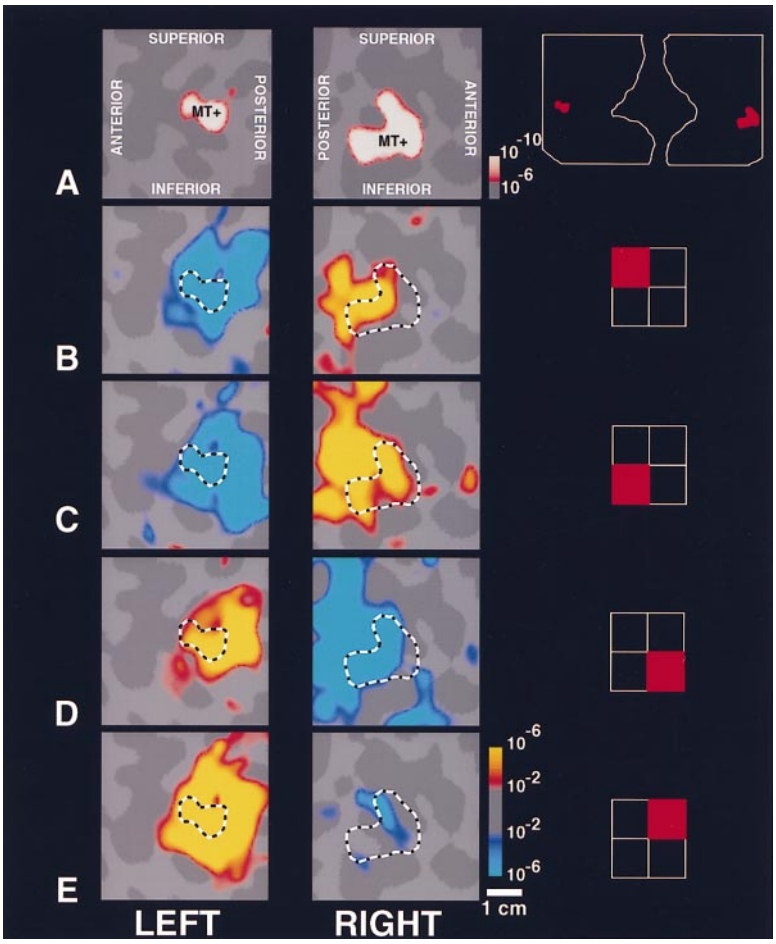

Figure 10. Attention-Related Activity in Area MT+ Is Lateralized but Not Otherwise Retinotopic

Each of the left and right columns shows a common region from the left and right hemisphere (respectively) from one subject. The cortex is relatively magnified in the panels (see calibration bar). (A) shows the activity produced during a scan comparing moving versus stationary stimuli. This revealed the location of human area MT+, as conventionally defined (red-through-white pseudocolor in the panels and red patches in the logo of the corresponding hemispheres to the right). The location of conventional brain axes (superior–inferior, anterior–posterior) is also shown, relative to the flattened topography. (B) through (E) show the selective activity produced by attention to a target in one quadrant, relative to that in other quadrants, as in Figures 4 and 6–8.

above tests for retinotopy and lateralization and (2) regions that did not. Included in the first set would be MT+ and the extrastriate retinotopic areas (e.g., V3A, V7, V8, V4v, etc.), centered at eccentricities near 10.5°–11°. The second set of cortical regions would include V1 and the extrastriate areas at eccentricities more central than that of the targets.

Recall that the first set of cortical regions showed these spatially selective MR increases only during one (or two, in the case of MT+) quadrant(s) of the four tested, and MR decreases also occurred when attention was directed to other quadrants (e.g., Figures 9–11). Thus, one would expect little net effect in the first set of cortical regions when the results from all the "attend" conditions were combined together. This expectation is generally confirmed in Figure 12A: higher-tier extrastriate cortical regions at the retinotopic projection of the targets did show little net decrease in activity.

Instead, the prominent MR decreases were found throughout the second cortical subdivision (V1 and foveal extrastriate representations), which did not show the pronounced MR increases in the selective attention comparisons described above. Thus, this data poses no discrepancy relative to the attention-related MR increases described in Figures 4 and 6–9.

To further clarify these surprising MR decreases, we sampled the time course from foveal V1 and V2, plus V3/VP, in subjects who also were shown a uniform gray baseline condition in addition to the main attention paradigm. Those results are shown in Figure 12B. The salient result is that attention to a given target in the (peripheral) visual field produced consistent MR decreases at the representation of more central eccentricities. Such MR effects represented decreases relative to the passive viewing epochs, when the visual stimulation was identical to that during the "attend" conditions. Furthermore, the MR levels during the attention task were even lower than MR levels when subjects viewed only a uniformly gray screen. An analogous t test of the data across subjects ($n = 6$) confirmed the decreased MR levels in central V1, V2, and V3/VP during spatial attention to these peripheral targets (mean MR modulation = 0.64%, $p < 0.001$).

Discussion

The comparisons between attention to one target versus attention to another showed very clear retinotopy, in the form of increased MR signals at the cortical sites to which the targets projected. The fact that MR signals increased (rather than decreased) during spatial attention is consistent with single unit studies in behaving macaques, which showed correspondingly higher firing

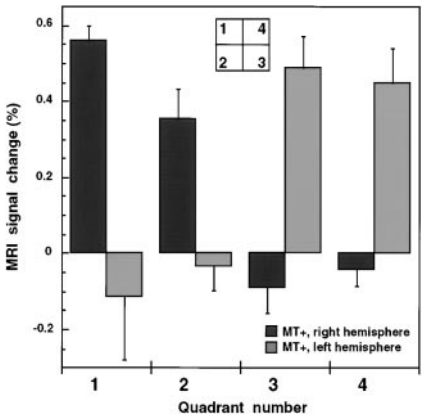

Figure 11. Group Data, Averaged across Subjects (n = 6), Confirms the Lateralization of Activity in Area MT+

The gray bars show the activity produced in MT+ within the left hemisphere; the black bars show the corresponding activity in the right hemisphere. Zero on the y axis represents the averaged MR level in MT+ during passive viewing of the same stimuli. MR signals increased in the right hemisphere when attention was directed to both upper and lower quadrants on the contralateral (left) side and vice versa (see logo in the upper left). This averaged data also showed consistent decreases in MT+ when attention was directed to either of the ipsilateral quadrants. The error bars represent the standard error.

rates during sustained attention to a given spatial location (e.g., Moran and Desimone, 1985; Luck et al., 1997).

The attention-based retinotopy was approximately as precise as that revealed in the (sensory-based) retinotopic maps (e.g., Figures 4 and 6–9). Such a finding implies that spatial attention uses some of the same receptive field mechanisms as the sensory-based retinotopic map. However, it could be argued that the similarity in attention-based versus sensory-based retinotopy is more fortuitous than fundamental, because there is no common basis for equating the activity produced in the two types of experiments. Though we cannot rule out this argument completely, we did not format our data in any unusual or preconceived manner for either the sensory-based or the attention-based maps. An even more persuasive counterargument was the dramatic increase in the cortical point spread in presumptively higher-tier areas (e.g., V3A and V7) compared to that in lower-tier areas (e.g., V1). This difference in cortical point spread occurred in both the sensory-based maps (Figure 3A; see also Figure 11 of Tootell et al., 1997) and the attention-based maps (e.g., Figures 4, 6, and 7), which strongly supports the idea of common underlying receptive field substrates.

On the face of it, our results supported the hierarchical model of spatial attention processing, which predicts higher attentional activity in extrastriate cortical areas compared to striate cortex. Selective attention was usually absent in V1 in our activity maps (e.g., Figures 4 and 6–8), and it was correspondingly smaller than that seen in extrastriate areas when our data was signal averaged across subjects, hemispheres, and upper/lower representations (Figure 9). These results are generally consistent with the relative size of attentional modulation reported in single units from V1, V2, and V4d of macaque (Moran and Desimone, 1985; Luck et al., 1997) and with human neuroimaging studies (Mangun et al., 1993; Heinze et al., 1994; Mangun, 1995; Clark and Hillyard, 1996; Woldorff et al., 1997). However, those studies did not systematically test for attention effects in each of the retinotopic areas we sampled.

However, it could be that we found such small effects in V1 only because our stimuli were too small (width = 0.4°) to produce robust hemodynamic effects in one or more voxels in V1. The relatively larger receptive fields in extrastriate cortical areas might produce more significantly activated voxels in response to the same small stimuli. A similar complication made it impossible to judge whether spatial attention was operating in the small receptive fields in macaque V1 (Moran and Desimone, 1985; Luck et al., 1997). However, those authors also noted that (unlike V2 and V4) attention-related increases in baseline firing did not occur in V1, which is at least consistent with the small size of our V1 effects (~0.13% activation).

It might seem surprising that we obtained prominent and lateralized effects in human MT+ based on attention to stationary targets. However, human MT+ does respond fairly well to flickering stationary stimuli (Tootell et al., 1995a) similar to those used in this study. Also, the infrequent shifts between horizontal and vertical bar orientations caused a subtle percept of illusory rotational stimulus motion. Prominent attention-related effects may also be an intrinsic feature of macaque MT (Treue and Maunsell, 1996) and human MT+ (Corbetta et al., 1991; Beauchamp et al., 1997; O'Craven et al., 1997).

Our more sensitive retinotopic maps revealed a new retinotopic area, which we call "V7," located just anterior to V3A. V7 showed quite robust activity during the present experiments on spatial attention (e.g., Figures 6, 7, and 9). V7 also appears to have been preferentially activated in a previous experiment on spatial attention (Culham et al., 1998), although the retinotopic mapping was less certain in that study. However, it should be noted that area V7 responds to a wide range of different stimuli, as do most visual areas.

Prior human neuroimaging studies have suggested that spatial attention per se (relative to passive viewing or other types of attention) preferentially activates parietal cortical regions (Haxby et al., 1994; Corbetta et al., 1993, 1995; Culham et al., 1998). Our spatially selective attention effects were prominent in areas MT+ and V3A (Figures 6–11), and these areas are likely connected with the parietal ("where") stream. However, we did not find prominent or widespread activation in parietal cortex during spatial attention per se (i.e., relative to passive viewing conditions; Figure 12A). This discrepancy may be due to the fact that stimuli in previous studies were shifting or moving, whereas those in our study remained in the same spatial location throughout each analyzed epoch. Thus, the lack of preferential activation in parietal cortex here supports the original hypothesis that parietal cortical activity is selective for shifts in spatial attention rather than activity due to spatial attention per se (Wurtz et al., 1980; Posner et al., 1984; Posner, 1988).

Among the most unexpected features of spatial attention per se (relative to passive viewing of the same stimulus) was the prominent decrease in MR levels during

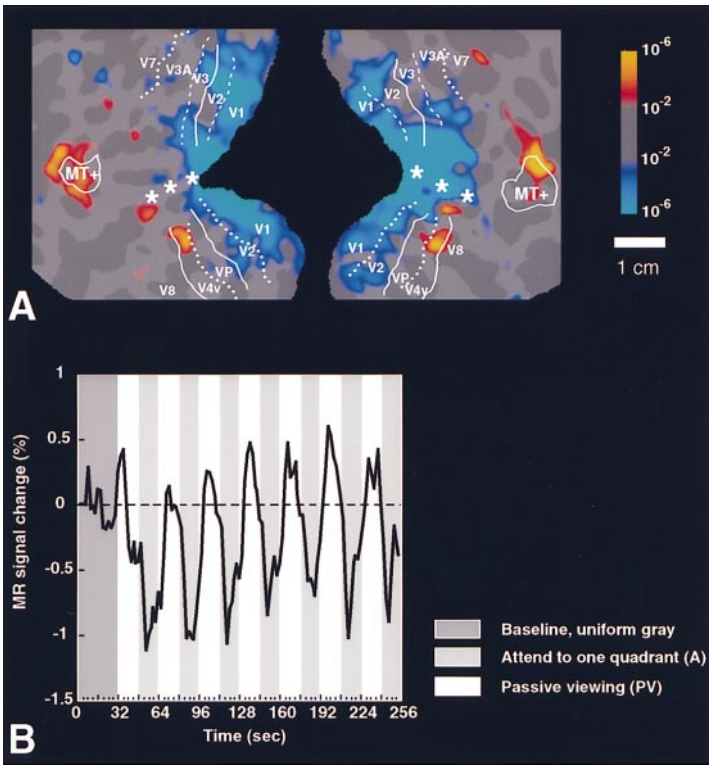

Figure 12. Spatial Attention Produces Decreased MR Levels in Cortical Representations Central to the Extrastriate Projection of the Bar Targets

(A) is the map of activity during attention to all four quadrants (i.e., all "A" epochs in Figure 1), minus the activity during the alternating passive viewing epochs ("PV" in Figure 1), in one subject. This comparison yielded MR signals, which were lower (blue-through-cyan pseudocolor) during the attention conditions than during passive viewing. This "negative" activity was typically centered on the foveal representation of V1, V2, and V3/VP, as in the right hemisphere of this figure. The MR-negative activity extended into the representation of the bar targets in area V1, but it avoided the representation of the bar targets in progressively higher areas (e.g., V3A, V7, V8, V4v, etc.). This pattern is presumably related to the progressively stronger attention-related MR increases in these same areas (see Figures 4 and 6–8). To clarify this topographic relationship, we placed the visual area names where the retinotopic representations of the bar targets were located. Little attention-related activity was produced in parietal cortex (outermost upper portions of each hemisphere).

(B) shows the time course of this MR activity at the representation of eccentricities closer than the attended target. The time course was acquired from all voxels showing statistically significant ($p < 10^{-5}$) modulation (of either polarity, from the attention versus passive viewing comparison) from areas V1, V2, and V3/VP, from the representation of eccentricities central to that of the target(0°–2°), from two subjects (four hemispheres). During the first 6 s, the MR signal had not yet stabilized, so that time period has been discarded from analysis. During the remainder of the first epoch (dark gray column), subjects viewed a uniform gray field. Thereafter, the bar targets appeared in alternating epochs as described in Figure 1. Subjects either attended to targets in a cued quadrant ("A," light gray columns), or passively viewed the same stimulus ("PV," white columns), as described in Figure 1. The average MR level during the first epoch (without the bar targets) was normalized to 100% (0% change). The introduction of the bar targets to the passive viewing condition (white columns) increased MR levels slightly. However, during the "attention" epochs, MR levels consistently decreased, relative to both the passive viewing of equivalent stimuli and even the average MR levels acquired prior to the introduction of the bar targets.

spatial attention, at the representation of eccentricities more central than that of the stimulus targets (e.g., Figure 12). Similar MR decreases in neuroimaging activity have been reported previously in the foveal representation (Paus et al., 1995; Tootell et al., 1998a). Such effects could reflect saccadic suppression (e.g., Duffy and Burchfiel, 1975), the increased "effort" required to inhibit eye movements toward peripherally presented targets when attention is directed more peripherally. Several examples in this study (Figures 3A, 4, and 12A) are consistent with this interpretation.

Other evidence suggests that these decreases may be part of a more general mechanism in which blood flow (and perhaps neural activity) is decreased at some cortical distance away from the locus of attention. This interpretation is strongly supported by the consistent decreases in MR signal when attention was directed to retinotopic locations different from those of the target (Figures 9–11). In unpublished experiments, we have also found that when subjects are instructed to fixate the center of a very small, foveally presented stimulus, a ring of decreased MR signal is found at more peripheral representations—exactly the inverse pattern compared to that in the "foveal inhibition" examples considered above. Furthermore, such blood flow decreases surrounding the site of cortical increases are not specific to visual cortex; similar attention-dependent effects were also reported in somatosensory cortex (Drevets et al., 1995). All this suggests that spatial attention may work by decreasing neural activity at nonattended locations, as well as increasing neural activity at the attended site. Similar models have been proposed earlier (Posner and Dehaene, 1994).

Experimental Procedures

General Procedures

The techniques used here were similar to those described elsewhere (Tootell et al., 1997; Hadjikhani et al., 1998). For the main experiments on spatial attention, eight normal human subjects, with emmetropic (or-corrected-to) vision, were scanned in a 3T General Electric MR scanner retrofitted with ANMR echoplanar imaging. MR images were acquired using a custom-built surface coil, yielding nearly uniform sensitivity bilaterally throughout the occipital and parietal lobes and the posterior portion of the temporal lobes. Voxels were 3.1 mm^2 in plane and 3–4 mm thick. Functional MR images were acquired using gradient echo sequences using a TE of 50 ms and 128 images/slice in 16 contiguous slices. The TR was either 4 s (retinotopic scans) or 2 s (all other scans). Thus, each scan lasted either 8 min 32 s or 4 min 16 s, respectively.

Most subjects were scanned in multiple sessions in order to provide test–retest data and to achieve adequate signal averaging of the smallest attention-related signals. Altogether, 152 scans (311,296 images) were acquired using our main spatial attention task from

eight subjects (see below). As many as 52 such scans (106,496 images) were obtained from a single subject, acquired across multiple scan sessions. Data from two subjects were not included in the quantitative analysis due to poor behavioral performance. For maximum comparability, most illustrations were taken from the two subjects from whom we acquired the most data (NH and JH). Directly related control scans of (1) phase-encoded retinotopy, (2) retinotopy of the main bar target stimuli, and (3) maps of nonretinotopic visual areas such as MT+ were also acquired from all subjects (65 additional scans, comprising 133,120 images). For comparison, similar visual area maps were also available from 42 additional subjects. Head motion was minimized by using bite bars with deep, individually molded dental impressions. These experiments were covered by Massachusetts General Hospital Human Studies Protocol numbers 90-7227 and 96-7464.

Main Attention Task and Stimuli

Subjects were instructed to steadily fixate the center of the stimulus throughout each scan. Throughout each scan, four bars appeared, one in each of the quadrants surrounding the central fixation point (see Figure 1A). In each quadrant, each bar was presented for 100 ms, followed by an interstimulus interval without a bar, followed by another bar presentation, and so on (see Figure 1B). Each interstimulus interval (200–500 ms) was chosen according to an equally weighted, random schedule, constrained within 50 ms increments. In each presentation, the bar appeared at either vertical or horizontal orientation, following a randomized schedule, with vertical orientations appearing nine times more often than horizontal orientations. Importantly, the timing of the bar presentations was calculated independently for each quadrant. The overall impression was a stream of four bars, presented rapidly and concurrently but nonsynchronously, at different orientations, in each quadrant.

Each bar was centered at an eccentricity of 10.5°–11°. The bars were presented at this relatively peripheral eccentricity for several reasons. First, this moved the representations of the bar locations as far as possible from each other, in both the visual field and the corresponding cortical maps. Second, this reduced the "blurring" of retinotopic fMRI patterns caused by unavoidable minor eye movements (e.g., microsaccades) during otherwise stable fixation. Third, according to subject reports, increasingly peripheral placement reduced the tendency to break fixation and look directly at the targets. The bars were made relatively long ($\sim 3° \times 0.4°$) so that their orientation could be spatially resolved at this eccentricity.

Each attention-related scan was comprised of 16 epochs, each 16 s long. In alternating epochs, subjects were cued to either attend to a single, specified quadrant (condition "A" in Figure 1C) or distribute their attention passively but evenly over all four bars (condition "PV" in Figure 1C). Within the "attend" conditions, the quadrants-to-be-attended were presented in random order.

Subjects were cued to begin passive viewing ("PV") by having all bars appear blue during a single, synchronized presentation 100 ms long. Subjects were cued to attend to bar orientation in a single quadrant (condition "A") by having one bar appear green (the quadrant to be attended), with the bars in the remaining three quadrants appearing red, during a single, synchronized presentation 100 ms long. After each synchronized bar presentation, the next bar presentation occurred 200–500 ms after the end of the cueing bar presentation, according to the randomized schedule described above.

The brief, synchronized cueing format ensured that subjects fixated the central point and divided their residual attention evenly across all four quadrants during the preceding passive viewing epochs: only by doing so could the subjects see which quadrant to attend to, accurately and consistently. Control tests showed that the minor difference in cue color produced no measurable effect on the patterns of fMRI activity. This lack of color artifact was not surprising, since a spatially unique color appeared at a given target location less than 0.1% of the time.

During each of the "attend" epochs, subjects pressed a button in the scanner every time they saw the bar-to-be-attended as horizontal. Responses were counted as correct only if they occurred within 700 ms following the initial frame of bar presentation, in (and only in) the quadrant to be attended. Responses occurring at any other time (including the passive viewing condition) were counted as incorrect. Performance on the task was monitored and calculated online. Feedback about performance accuracy (percent correct) was given to the subject after each scan, to boost motivation and improve performance. All subjects were motivated, experienced psychophysical subjects who were well trained on the task prior to MR acquisition and were frequently reminded to maintain fixation on the central point.

The task was designed to be difficult. With concentrated attention to a given location in the visual field, these subjects were typically able to achieve an accuracy of 70%–90% (chance performance = <8%). According to subject reports, the orientation changes occurring at nonattended targets were not salient enough to distract attention from the attended target. Subjects did this task during 8–19 scans (16,384–38,532 images) within a given scan session.

Retinotopic Control Stimuli I: Bar Targets versus Uniform Gray

In additional scans, we presented stimuli designed to reveal the retinotopic location of the bar targets themselves. In those control scans, subjects fixated the center of the flashing four-bar stimulus in 16 s epochs (as in the "PV" condition in Figure 1C) in alternation with 16 s views of a uniform gray, excepting the fixation point. Subjects normally did two scans (4,096 images) of such stimuli in each scan session.

Retinotopic Control Stimuli II: Phase-Encoded Mapping

To confirm the retinotopic location of the bar targets, and to reveal the location of the retinotopic visual areas, we also did phase-encoded retinotopic mapping in each subject, in additional scans. To map the (relatively crude) retinotopy in the most anterior areas of human visual cortex, extensive signal averaging and several new procedures (described by Hadjikhani et al., 1998) were implemented. The sum of all these manipulations produced very robust retinotopic maps.

Since the retinotopic signal averaging required 1–2 hr of scanning, we usually acquired the retinotopic data in different scan sessions than those in which the attention data was acquired.

Though these retinotopic control stimuli (I and II, above) are typical of contemporary retinotopic mapping approaches, it could be argued that such tests cannot fully exclude attention-related contributions from exogenously driven spatial attention, driven by the spatially varying stimuli. However, such arguments are less persuasive after one has viewed a few cycles of these repetitive retinotopic stimuli. Furthermore, our main manipulations of attention (above) manipulated endogenously driven spatial attention, without any stimulus differences between the different experimental conditions that could produce artifacts due to exogenous attention.

Data Analysis

The visual areas analyzed here were: V1, V2, V3/VP, V3A, V4v, MT+, V7, and V8. Areas V1, V2, and V3/VP have been described based on retinotopic criteria in many previous reports (e.g., Schneider et al., 1993; DeYoe et al., 1996; Sereno et al., 1995; Tootell et al., 1995a, 1995b, 1996, 1997, 1998a, 1998b; Engel et al., 1997). Area V3A was described by Tootell et al. (1997), and V8 was described by Hadjikhani et al. (1998). Area V4v has been described in Sereno et al. (1995), DeYoe et al. (1996), Tootell et al. (1997), and Hadjikhani et al. (1998). Area V7 was described briefly in Tootell et al. (1998b), and it is discussed more fully here. Area "MT+" was based on additional scans comparing moving versus stationary stimuli, as in prior reports (Lueck et al., 1989; Zeki et al., 1991; Watson et al., 1993; Dupont et al., 1994; McCarthy et al., 1995; Tootell et al., 1995a, 1995b).

Except for the increased signal averaging, the data analysis was similar to that described elsewhere (Tootell et al., 1997; Hadjikhani et al., 1998). Statistical maps were calculated using one of two methods, depending on the type of comparison made. For periodic stimulus manipulations (e.g., retinotopic mapping and two-conditions comparisons), a fast Fourier transform was performed on the time course of each voxel. Then, the ratio of the signal power at the fundamental stimulus frequency and average power at all frequencies was computed, excluding the first and second harmonics and very low frequencies (1–3 cycles per scan). Under the assumption

of white (temporally uncorrelated) noise, the power at each frequency is an independent, identically distributed χ^2 random variable, and so the resulting ratio of signal power is F distributed. On this basis, the significance of the activation at each voxel was determined using an F statistic.

In the main attention experiment (e.g., Figure 1), which compared multiple conditions in randomized epochs, the statistical significance maps were computed using linear regression analysis. The fMRI signal was modeled as a linear convolution of a hemodynamic impulse function (a γ function with typical parameters; e.g., Dale and Buckner, 1997), with a neuronal activation function that was assumed to be constant during each epoch. The activation amplitude for each condition was estimated from the fMRI time course at each voxel, by fitting the fMRI signal model to the observed time course. The significance of the difference between the activation amplitudes of different conditions was computed using a standard t statistic.

In several across-subject analyses, MR time courses were extracted from voxels within specified visual areas and/or within eccentricity-bounded portions of specific visual areas. The linear regression estimates of percent signal change for different conditions were then averaged within each ROI for each subject. Finally, these ROI-based averages were compared statistically, as described in the text.

Acknowledgments

These experiments were supported by NEI grant #EY07980 to R. B. H. T. and HFS grants to R. B. H. T. and A. M. D. We thank Ewa Wojciulik and Jody Culham for collaborating on informative pilot experiments related to the present study. We thank Bruce Fischl, Anthony Wagner, and Arthur Liu for crucial assistance with the data analysis. We thank Greg Simpson, Jack Belliveau, and Marty Woldorff for helpful suggestions on stimulus design and attention-related issues. We thank Terrance Campbell, Tim Reese, and Bruce Rosen for MRI support and the Rowland Institute for specialized machining.

Received August 10, 1998; revised November 23, 1998.

References

Aine, C.J., Supek, S., and George, J.S. (1995). Temporal dynamics of visual-evoked neuromagnetic sources: effects of stimulus parameters and selective attention. Int. J. Neurosci. *80*, 79–104.

Andersen, R.A., Asanuma, C., and Cowan, W.M. (1985a). Callosal and prefrontal associational projecting cell populations in area 7A of the macaque monkey: a study using retrogradely transported fluorescent dyes. J. Comp. Neurol. *232*, 443–455.

Andersen, R.A., Essick, G.K., and Siegel, R.M. (1985b). Encoding of spatial location by posterior parietal neurons. Science *230*, 456–458.

Beauchamp, M.S., Cox, R.W., and DeYoe, E.A. (1997). Graded effects of spatial and featural attention on human area MT and associated motion processing areas. J. Neurophysiol. *78*, 516–520.

Boussaoud, D., Desimone, R., and Ungerleider, L.G. (1991). Visual topography of area TEO in the macaque. J. Comp. Neurol. *306*, 554–575.

Clark, V.P., and Hillyard, S.A. (1996). Spatial selective attention affects early extrastriate but not striate components of the visual evoked potential. J. Cogn. Neurosci. *8*, 387–402.

Clarke, S., and Miklossy, J. (1990). Occipital cortex in man: organization of callosal connections, related myelo- and cytoarchitecture, and putative boundaries of functional visual areas. J. Comp. Neurol. *298*, 188–214.

Colby, C.L. (1991). The neuroanatomy and neurophysiology of attention. J. Child Neurol. *6* (suppl.), S90–S118.

Connor, C.E., Preddie, D.C., Gallant, J.L., and Van Essen, D.C. (1997). Spatial attention effects in macaque area V4. J. Neurosci. *17*, 3201–3214.

Corbetta, M., Miezin, F.M., Dobmeyer, S., Shulman, G.L., and Petersen, S.E. (1991). Selective and divided attention during visual discriminations of shape, color, and speed: functional anatomy by positron emission tomography. J. Neurosci. *11*, 2383–2402.

Corbetta, M., Miezin, F.M., Shulman, G.L., and Petersen, S.E. (1993). A PET study of visuospatial attention. J. Neurosci. *13*, 1202–1226.

Corbetta, M., Shulman, G.L., Miezin, F.M., and Petersen, S.E. (1995). Superior parietal cortex activation during spatial attention shifts and visual feature conjunction. Science *270*, 802–805.

Crick, F. (1984). Function of the thalamic reticular complex: the searchlight hypothesis. Proc. Natl. Acad. Sci. USA *81*, 4586–4590.

Culham, J.C., Brandt, S.A., Cavanagh, P., Kanwisher, N.G., Dale, A.M., and Tootell, R.B.H. (1998). Cortical fMRI activation produced by attentive tracking of moving targets. J. Neurophysiol. *80*, 2657–2665.

Dale, A.M., and Buckner, R.L. (1997). Selective averaging of rapidly presented individual trials using fMRI. Hum. Brain Map. *5*, 326–340.

Desimone, R., and Duncan, J. (1995). Neural mechanisms of selective visual attention. Annu. Rev. Neurosci. *18*, 193–222.

DeYoe, E.A., Carman, G.J., Bandettini, P., Glickman, S., Wieser, J., Cox, R., Miller, D., and Neitz, J. (1996). Mapping striate and extrastriate visual areas in human cerebral cortex. Proc. Natl. Acad. Sci. USA *93*, 2382–2386.

Drevets, W.C., Burton, H., Videen, T.O., Snyder, A.Z., Simpson, J.R., Jr., and Raichle, M.E. (1995). Blood flow changes in human somatosensory cortex during anticipated stimulation [see comments]. Nature *373*, 249–252.

Duffy, F.H., and Burchfiel, J.L. (1975). Eye movement–related inhibition of primate visual neurons. Brain Res. *89*, 121–132.

Dupont, P., Orban, G.A., DeBruyn, B., Verbruggen, A., and Mortelmans, L. (1994). Many areas in the human brain respond to visual motion. J. Neurophysiol. *72*, 1420–1424.

Engel, S.A., Glover, G.H., and Wandell, B.A. (1997). Retinotopic organization in human visual cortex and the spatial precision of functional MRI. Cereb. Cortex *7*, 181–192.

Eriksen, C.W., and Hoffman, J.E. (1973). The extent of processing of noise elements during selective encoding from visual display. Percept. Psychophys. *14*, 155–160.

Felleman, D.J., and Van Essen, D.C. (1991). Distributed hierarchical processing in the primate cerebral cortex. Cereb. Cortex *1*, 1–47.

Gattass, R., Sousa, A.P., and Gross, C.G. (1988). Visuotopic organization and extent of V3 and V4 of the macaque. J. Neurosci. *8*, 1831–1845.

Hadjikhani, N., Liu, A.K., Dale, A.M., Cavanagh, P., and Tootell, R.B.H. (1998). Retinotopy and color selectivity in human visual cortical area V8. Nat. Neurosci. *1*, 235–241.

Haxby, J.V., Horwitz, B., Ungerleider, L.G., Maisog, J.M., Pietrini, P., and Grady, C.L. (1994). The functional organization of human extrastriate cortex: a PET–rCBF study of selective attention to faces and locations. J. Neurosci. *14*, 6336–6353.

Heinze, H.J., Mangun, G.R., Burchert, W., Hinrichs, H., Scholz, M., Munte, T.F., Gos, A., Scherg, M., Johannes, S., Hundeshagen, H., et al. (1994). Combined spatial and temporal imaging of brain activity during visual selective attention in humans. Nature *372*, 543–546.

Luck, S.J., Chelazzi, L., Hillyard, S.A., and Desimone, R. (1997). Neural mechanisms of spatial selective attention in areas V1, V2, and V4 of macaque visual cortex. J. Neurophysiol. *77*, 24–42.

Lueck, C.J., Zeki, S., Friston, K.J., Deiber, M.P., Cope, P., Cunningham, V.J., Lammertsma, A.A., Kennard, C., and Frackowiak, R.S. (1989). The colour centre in the cerebral cortex of man. Nature *340*, 386–389.

Mangun, G.R. (1995). Neural mechanisms of visual selective attention. Psychophysiology *32*, 4–18.

Mangun, G.R., Hillyard, S.A., and Luck, S.J. (1993). Electrocortical substrates of visual selective attention. In Attention and Performance XIV. D. Meyer and S. Kornblum, eds. (Cambridge, MA, MIT Press), pp. 219–244.

Mangun, G.R., Hopfinger, J., Kussmaul, C.L., Fletchert, E., and Heinze, H.J. (1997). Covariations in ERP and PET measures of spatial selective attention in human extrastriate visual cortex. Hum. Brain Map. *5*, 273–279.

Maunsell, J.H. (1995). The brain's visual world: representation of visual targets in cerebral cortex. Science *270*, 764–769.

May, J.G., and Andersen, R.A. (1986). Different patterns of corticopontine projections from separate cortical fields within the inferior parietal lobule and dorsal prelunate gyrus of the macaque. Exp. Brain Res. *63*, 265–278.

McCarthy, G., Spicer, M., Adrignolo, A., Luby, M., Gore, J., and Allison, T. (1995). Brain activation associated with visual motion studied by functional magnetic resonance imaging in humans. Hum. Brain Map. *2*, 234–243.

Moran, J., and Desimone, R. (1985). Selective attention gates visual processing in the extrastriate cortex. Science *229*, 782–784.

Motter, B.C. (1993). Focal attention produces spatially selective processing in visual cortical areas V1, V2, and V4 in the presence of competing stimuli. J. Neurophysiol. *70*, 909–919.

Nobre, A.C., Sebestyen, G.N., Gitelman, D.R., Mesulam, M.M., Frackowiak, R.S., and Frith, C.D. (1997). Functional localization of the system for visuospatial attention using positron emission tomography. Brain *120*, 515–533.

O'Craven, K.M., Rosen, B.R., Kwong, K.K., Treisman, A., and Savoy, R.L. (1997). Voluntary attention modulates fMRI activity in human MT–MST. Neuron *18*, 591–598.

Paus, T., Marrett, S., Worsley, K.J., and Evans, A.C. (1995). Extraretinal modulation of cerebral blood flow in the human visual cortex: implications for saccadic suppression. J. Neurophysiol. *74*, 2179–2183.

Posner, M.I. (1988). Structures and functions of selective attention. In Master Lectures in Clinical Neurpsychology, T. Boll and B. Bryant, eds. (Washington, DC: American Psychiatric Association), pp. 173–202.

Posner, M.I., and Dehaene, S. (1994). Attentional networks. Trends Neurosci. *17*, 75–79.

Posner, M.I., and Petersen, S.E. (1990). The attention system of the human brain. Annu. Rev. Neurosci. *13*, 25–42.

Posner, M.I., Snyder, C.R., and Davidson, B.J. (1980). Attention and the detection of signals. J. Exp. Psychol. *109*, 160–174.

Posner, M.I., Walker, J.A., Friedrich, F.J., and Rafal, R.D. (1984). Effects of parietal injury on covert orienting of attention. J. Neurosci. *4*, 1863–1874.

Roelfsema, P.R., Lamme, V.A.F., and Spekreijse, H. (1998). Object-based attention in primary visual cortex of the macaque monkey. Nature, in press.

Schneider, W., Noll, D.C., and Cohen, J.D. (1993). Functional topographic mapping of the cortical ribbon in human vision with conventional MRI scanners. Nature *365*, 150–153.

Sereno, M.I., Dale, A.M., Reppas, J.B., Kwong, K.K., Belliveau, J.W., Brady, T.J., Rosen, B.R., and Tootell, R.B.H. (1995). Borders of multiple visual areas in humans revealed by functional magnetic resonance imaging. Science *268*, 889–893.

Shulman, G.H., Corbetta, M., Buckner, R.L., Raichle, M.E., Fiez, J.A., Miezen, F.M., and Petersen, S.E. (1997). Top-down modulation of early sensory cortex. Cereb. Cortex *7*, 193–206.

Tootell, R.B., Reppas, J.B., Kwong, K.K., Malach, R., Born, R.T., Brady, T.J., Rosen, B.R., and Belliveau, J.W. (1995a). Functional analysis of human MT and related visual cortical areas using magnetic resonance imaging. J. Neurosci. *15*, 3215–3230.

Tootell, R.B., Reppas, J.B., Dale, A.M., Look, R.B., Sereno, M.I., Malach, R., Brady, T.J., and Rosen, B.R. (1995b). Visual motion aftereffect in human cortical area MT revealed by functional magnetic resonance imaging. Nature *375*, 139–141.

Tootell, R.B., Dale, A.M., Sereno, M.I., and Malach, R. (1996). New images from human visual cortex. Trends Neurosci. *19*, 481–489.

Tootell, R.B., Mendola, J.D., Hadjikhani, N.K., Ledden, P.J., Liu, A.K., Reppas, J.B., Sereno, M.I., and Dale, A.M. (1997). Functional analysis of V3A and related areas in human visual cortex. J. Neurosci. *17*, 7060–7078.

Tootell, R.B., Mendola, J.D., Hadjikhani, N.K., Liu, A.K., and Dale, A.M. (1998a). The representation of the ipsilateral visual field in human cerebral cortex. Proc. Natl. Acad. Sci. USA *95*, 818–824.

Tootell, R.B.H., Hadjikhani, N.K., Mendola, J.D., Marrett, S., and Dale, A.M. (1998b). From retinotopy to recognition: fMRI in human visual cortex. Trends Cogn. Sci. *2*, 174–183.

Treisman, A., and Gormican, S. (1988). Feature analysis in early vision: evidence from search asymmetries. Psychol. Rev. *95*, 15–48.

Treue, S., and Maunsell, J.H. (1996). Attentional modulation of visual motion processing in cortical areas MT and MST. Nature *382*, 539–541.

Vandenberghe, R., Dupont, P., DeBruyn, B., Bormans, G., Michiels, J., Mortelmans, L., and Orban, G.A. (1996). The influence of stimulus location on the brain activation pattern in detection and orientation discrimination. Brain *119*, 1263–1276.

Van Essen, D.C., and Zeki, S.M. (1978). The topographic organization of rhesus monkey prestriate cortex. J. Physiol. (Lond.) *277*, 193–226.

Watanabe, T., Sasaki, Y., Miyauchi, S., Putz, B., Fujimaki, N., Nielsen, M., Takino, R., and Miyakawa, S. (1998). Attention-regulated activity in human primary visual cortex. J. Neurophysiol. *79*, 2218–2221.

Watson, J.D.G., Myers, R., Frackowiak, R.S.J., Hajnal, J.V., Woods, R.P., Mazziota, J.C., Shipp, S., and Zeki, S. (1993). Area V5 of the human brain: evidence from a combined study using positron emission tomography and magnetic resonance imaging. Cereb. Cortex *3*, 79–94.

Woldorff, M.G., Fox, P.T., Matzke, M., Lancaster, J.L., Veeraswamy, S., Zamarripa, F., Seabolt, M., Glass, T., Gao, J.H., Martin, C.C., and Jerabek, P. (1997). Retinotopic organization of early visual spatial attention effects as revealed by PET and ERPs. Hum. Brain Map. *5*, 280–286.

Wurtz, R.H., Goldberg, M.E., and Robinson, D.L. (1980). Behavioral modulation of visual responses in monkeys. Prog. Psychobiol. Physiol. Psychol. *9*, 42–83.

Zeki, S., Watson, J.D.G., Lueck, C.J., Friston, K.J., Kennard, C., and Frackowiak, R.S.J. (1991). A direct demonstration of functional specialization in human visual cortex. J. Neuroscience *11*, 641–649.